SIAM J. NUMER. ANAL.
Vol. 46, No. 6, pp. 2953–2977

ENO MULTIRESOLUTION SCHEMES WITH GENERAL DISCRETIZATIONS*

PASCAL GETREUER† AND FRANÇOIS G. MEYER‡

Abstract. Harten's framework is a nonlinear generalization of the wavelet framework. Previously, the choice of discretization (scaling function) in Harten multiresolution schemes has been limited to point-value, cell-average, and hat-based discretization. This paper shows how to construct multiresolution schemes consistent with Harten's framework for a variety of discretizations. The construction here begins with the discrete operators and deduces the corresponding continuous operators, reversing the order of the usual approach. This construction yields as a special case essentially nonoscillatory (ENO) multiresolution schemes for any order of spline discretization and also has the flexibility to define multiresolution schemes with nonspline discretizations. An error-control strategy is also developed.

Key words. ENO interpolation, multiscale decomposition, wavelets

AMS subject classifications. 41A05, 65D05, 65N55, 42C40

DOI. 10.1137/060663763

1. Introduction.

Harten's multiresolution framework [5] generalizes wavelet transforms. Harten's framework requires that the decimation (coarsening) operator be linear, but the prediction (refining) operator may be nonlinear.

One effective choice for this prediction operator is essentially nonoscillatory (ENO) interpolation, an edge-adaptive interpolation technique originating in the numerical methods of hyperbolic conservation laws [12]. ENO multiresolution schemes based on ENO interpolation achieve efficient, edge-adaptive decompositions and are especially successful on piecewise-smooth functions, as shown by the numerical experiments in [2].

1.1. Earlier work.

Much work on nonlinear multiresolution in the wavelet literature has been inspired by Sweldens's wavelet lifting scheme [19]. In [8], Claypoole et al. used a nonlinear prediction stage to create an edge-adaptive transform. Heijmans and Goutsias [15] developed the general morphological wavelets framework for constructing nonlinear wavelets.

Many have worked to develop Harten multiresolution, including:

- Harten [13, 14] developed the foundation of Harten's framework and ENO multiresolution schemes.
- Cohen, Dyn, and Mateï [10] studied the convergence of ENO prediction schemes and other properties of recursive prediction using the machinery of subdivision refinement schemes.
- Sonar, Iske, Cecil, Qian, and Osher [7, 16, 18] proposed the extensions of ENO beyond one dimension using radial basis functions. Cohen and Mateï [9] extended ENO to two dimensions with rotating step functions.

*Received by the editors June 27, 2006; accepted for publication (in revised form) March 28, 2008; published electronically August 20, 2008. This work was supported by National Science Foundation VIGRE grant DMS-9810751.

http://www.siam.org/journals/sinum/46-6/66376.html

†Department of Mathematics, University of California Los Angeles, Los Angeles, CA 90095 (getreuer@gmail.com).

‡Department of Electrical Engineering, University of Colorado at Boulder, Boulder, CO 80309 (francois.meyer@colorado.edu).

- Aràndiga, Donat, and Harten [6] constructed an ENO transform satisfying Harten's framework using hat-based discretization.

1.2. This paper's contribution. Harten's framework is in principle more general than the wavelet framework, yet most development so far has focused on the point-value and cell-average discretizations (analogous to the lazy and Haar wavelets). Aràndiga, Donat, and Harten [6] developed a third, the hat-based discretization. In wavelet nomenclature, only three possible scaling functions have been thoroughly considered.

The goal of this paper is to extend these constructions to all discretizations where the decimation filter is finite impulse response (FIR). This class of discretizations includes those induced by FIR wavelets as well as the three previously developed discretizations. Previously, Harten constructions start in the continuous domain by defining a discretization operator $\mathcal{D}_k$ and a reconstruction operator $\mathcal{R}_k$. Approaching the construction from the discrete domain, however, many operators can be defined without $\mathcal{D}_k$ and $\mathcal{R}_k$. We construct the decimation and prediction operators first and then deduce $\mathcal{D}_k$ and a choice of $\mathcal{R}_k$.

1.3. Outline. Section 2 reviews the construction of Harten's framework. Section 3 describes ENO interpolation (section 3.1), point-value discretization ENO schemes (section 3.2), and cell-average and hat-based discretization ENO schemes (section 3.3). Sections 4 and 5 develop for any FIR decimation filter h,

- a valid prediction operator (section 4.3),
- detail operators for a nonredundant scheme (section 4.1),
- $\mathcal{D}_k$ and $\mathcal{R}_k$ (section 4.4),
- an error-control strategy (section 5).

Section 6 develops two examples of this construction: Schemes with any spline discretization (section 6.1) and an example of nonspline discretization (section 6.2). Section 7 is the conclusion.

1.4. Notation. Define a *discrete signal* as any real or complex-valued sequence $v = (v_n)_{n\in\mathbb{Z}}$. An FIR filter is a discrete signal that is nonzero for finitely many n. Define its bilateral Z-transform $v(z)$,

$$v(z) \stackrel{\text{def}}{=} \mathcal{Z}\{v\}(z) = \sum_{n\in\mathbb{Z}} v_n z^{-n}. \tag{1.1}$$

Define dyadic downsampling and upsampling on v as

$$(\downarrow v)_n = v_{2n}, \qquad (\uparrow v)_n = \begin{cases} v_{n/2} & \text{if } n \text{ even}, \\ 0 & \text{if } n \text{ odd}. \end{cases}$$

The Z-transform of $\uparrow\downarrow v$ is

$$\tfrac{1}{2}\big(v(z) + v(-z)\big). \tag{1.2}$$

Denote by $\hat{\cdot}$ the Fourier transform,

$$\hat{f}(\omega) \stackrel{\text{def}}{=} \int_{-\infty}^{+\infty} f(x)\, \mathrm{e}^{-i\omega x}\, dx.$$

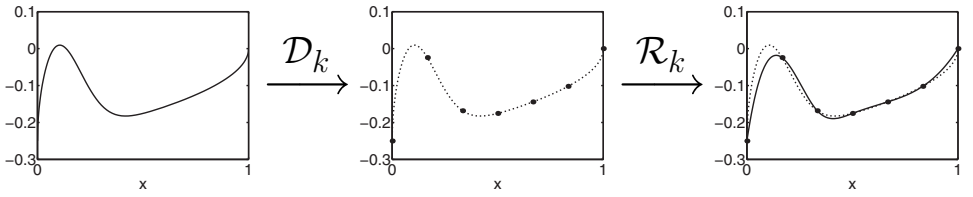

FIG. 2.1. *Left:* $f(x) = \mathrm{e}^{-25x^2}\sqrt{x} - \frac{1}{4}\sqrt{1-x}$. *Center:* $\mathcal{D}_k f$ *with point-value discretization,* $(\mathcal{D}_k f)_n = f(n/6)$. *Right:* $\mathcal{R}_k \mathcal{D}_k f$, *where* $\mathcal{R}_k$ *is cubic spline interpolation.*

2. Harten's framework. Harten's framework [5] builds from two operators: *Discretization* $\mathcal{D}_k$ and *reconstruction* $\mathcal{R}_k$. These operators map between functions and discrete signals at resolution k. The index k denotes the resolution level, where increasing k implies finer resolution.

Let $\mathcal{F}$ be space of functions, and let V^k be a vector space of discrete signals. Discretization $\mathcal{D}_k : \mathcal{F} \to V^k$ is a *linear* operator mapping $f \in \mathcal{F}$ to a discrete signal $v^k = \mathcal{D}_k f$. Reconstruction $\mathcal{R}_k : V^k \to \mathcal{F}$ is a (generally) *nonlinear* operator mapping discrete signals to functions. This nonlinearity is where Harten's framework is more general than the wavelet framework. Figure 2.1 shows an example of discretization and reconstruction, where $\mathcal{D}_k$ is point-value discretization and $\mathcal{R}_k$ is cubic spline interpolation.

Harten's framework requires that the discretization and reconstruction operators satisfy a consistency relationship

$$\mathcal{D}_k \mathcal{R}_k = I_{V^k}, \tag{2.1}$$

where I_{V^K} denotes identity on V^k. The reconstruction $\mathcal{R}_k v^k$ must be consistent with the discrete information in v^k.

To construct a multiresolution scheme, define a decimation operator $D_k^{k-1} = \mathcal{D}_{k-1}\mathcal{R}_k$ and a prediction operator $P_{k-1}^k = \mathcal{D}_k \mathcal{R}_{k-1}$ as follows:

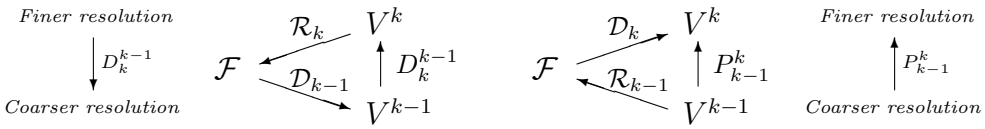

Decimation reduces the discrete signal v^k to v^{k-1}; $v^{k-1} = D_k^{k-1} v^k$. The prediction operator predicts v^k from v^{k-1}; $P_{k-1}^k v^{k-1}$ is an approximation of v^k. Define the prediction error as

$$e^k = v^k - P_{k-1}^k v^{k-1}.$$

The operators D_k^{k-1} and P_{k-1}^k can be used to construct a multiresolution pyramid (see Figure 2.2). If v^k is the input, then one stage of decomposition outputs the

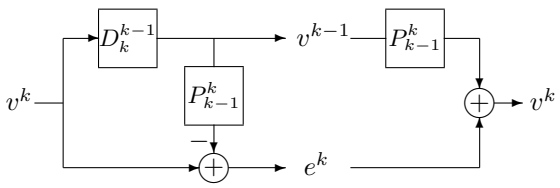

FIG. 2.2. *Pyramid decomposition under Harten's framework.*

decimated signal v^{k-1} and the prediction error e^k. Because e^k is at the same sample rate as v^k, the decomposition is 50% oversampled, that is, (v^{k-1}, e^k) redundantly represents v^k. This single decomposition stage is iterated on the decimated signal for a multiresolution representation $(v^{k-L}, e^{k-L+1}, \dots, e^k)$.

The discretization sequence $(\mathcal{D}_k)$ is *nested* if

$$\mathcal{D}_k f = 0 \;\Rightarrow\; \mathcal{D}_{k-1} f = 0 \qquad \text{for all } f \in \mathcal{F},\ k \in \mathbb{Z}. \tag{2.2}$$

If $(\mathcal{D}_k)$ is nested, then D^k_{k-1} has no dependence on $\mathcal{R}_k$ despite its definition, and it must be a linear operator [5]. This property, along with the consistency requirement (2.1), implies that $\mathcal{D}_m \mathcal{R}_k \mathcal{D}_k = \mathcal{D}_m$ for $m \le k$ and a discrete analogy of the consistency relationship

$$D^{k-1}_k P^k_{k-1} = \mathcal{D}_{k-1}\mathcal{R}_k\mathcal{D}_k\mathcal{R}_{k-1} = \mathcal{D}_{k-1}\mathcal{R}_{k-1} = I_{V^{k-1}}. \tag{2.3}$$

Consequently, e^k is in the nullspace of D^{k-1}_k:

$$\begin{aligned} D^{k-1}_k e^k &= D^{k-1}_k \left(I_{V^k} - P^k_{k-1} D^{k-1}_k\right) v^k \\ &= \left(D^{k-1}_k - D^{k-1}_k (P^k_{k-1} D^{k-1}_k)\right) v^k \;=\; 0. \end{aligned} \tag{2.4}$$

By (2.4), it is possible to design a nonredundant (critically sampled) multiresolution decomposition. Let G_k be a detail encoder such that $d^k = G_k e^k$ is at half the sample rate of e^k, and let $\tilde{G}_k$ be the corresponding decoder such that $\tilde{G}_k G_k e^k = e^k$ for any e^k in the nullspace of D^{k-1}_k. Then (v^{k-1}, d^k) is a nonredundant representation of v^k. This single stage is iterated on the decimated signal for a multiresolution representation $(v^{k-L}, d^{k-L+1}, \dots, d^k)$.

In summary, a multiresolution scheme within Harten's framework is characterized by six operators: The fundamental discretization and reconstruction operators $\mathcal{D}_k$ and $\mathcal{R}_k$, the decimation operator D^{k-1}_k, the prediction operator P^k_{k-1}, and the detail operators G_k and $\tilde{G}_k$. The next section shows how ENO multiresolution schemes fit into the Harten framework.

3. ENO multiresolution schemes. ENO multiresolution schemes are Harten multiresolution schemes where the reconstruction operator is ENO interpolation. ENO interpolation is an effective edge-adaptive strategy for piecewise polynomial interpolation (essentially) without oscillatory artifacts (see Figure 3.1).

3.1. ENO interpolation. Let $v_n = f(x_n)$ be samples from an underlying function f. ENO interpolation approximates f from the point-values v by a piecewise polynomial model.

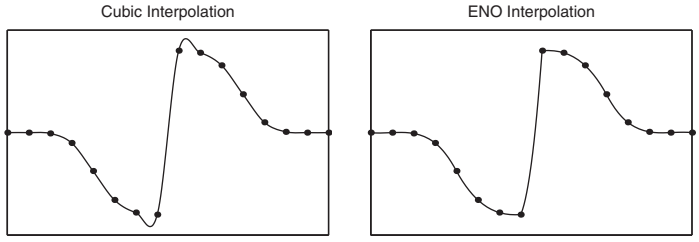

FIG. 3.1. *An interpolation of piecewise-smooth data. Cubic interpolation produces oscillations around the discontinuity, but ENO interpolation does not.*

On each subinterval $[x_{n-1}, x_n]$, a polynomial interpolant $q_n(x)$ is constructed based on a stencil $\mathcal{S}_n$ such that $q_n(x) = f(x)$ for all $x \in \mathcal{S}_n$. For example, cubic interpolation finds the cubic polynomial q_n satisfying the point-values at $\mathcal{S}_n = \{x_{n-2}, x_{n-1}, x_n, x_{n+1}\}$ to interpolate $[x_{n-1}, x_n]$. In ENO interpolation, the $\mathcal{S}_n$ are selected to adapt to the v^k.

The accuracy of such an interpolant depends heavily on the stencil. Let $\mathcal{S}$ be a stencil, and denote by $\widehat{\mathcal{S}}$ its convex hull. If $\mathcal{S}$ has $M+1$ points and $f \in C^{M+1}(\widehat{\mathcal{S}})$, the interpolation error is

$$f(x) - q(x) = \frac{f^{(M+1)}\big(\xi(x)\big)}{(M+1)!} \prod_{x_j \in \mathcal{S}} (x - x_j) \quad \text{for some } \xi(x) \in \widehat{\mathcal{S}}. \tag{3.1}$$

If f is locally smooth, the interpolation error is small. However, if f has a jump or derivative singularity in $\widehat{\mathcal{S}}$, the error can be much greater [5].

ENO interpolation attempts to choose stencils that do not cross jumps or derivative discontinuities. To construct an interpolant $q_n(x)$ of degree M, consider the stencils $\mathcal{S}_n = \{x_{k_n-1}, \ldots, x_{k_n+M-1}\}$, $n - M + 1 \le k_n \le n$. Each stencil has $M+1$ points and includes x_{n-1} and x_n. The interpolation error associated with a particular stencil is estimated with the Mth-order divided difference of the stencil samples $f[\mathcal{S}]$:

$$|f[\mathcal{S}]| = \begin{cases} 0, & f \text{ is locally polynomial,} \\ O([f^{(p)}])/h^{M-p}, & \text{the stencil crosses a discontinuity in } f^{(p)}, \\ O(\|f^{(M)}\|), & \text{otherwise,} \end{cases} \tag{3.2}$$

where $[f^{(p)}]$ is the size of the jump and $\|f^{(M)}\|$ is the max-norm of $f^{(M)}$ over $\widehat{\mathcal{S}}$. For example, if $M = 2$, (3.2) has the form

$$|f[\mathcal{S}_i]| = \frac{1}{2h^2} \left| f(x_{k-1}) - 2f(x_k) + f(x_{k+1}) \right|, \quad k = i-1 \text{ or } i.$$

This estimate distinguishes between intervals where f is locally linear and intervals containing jumps or first derivative discontinuities. In general, the Mth-order error estimate can detect discontinuities in up to the $M-1$ derivative.

In [12], Harten et al. consider two methods for choosing the stencil shifts k_n:

Hierarchical stencil selection

For each n
  $k_n := n$
  for $j = 0, \ldots, M-2$
    if $|f[x_{k_n-2}, \ldots, x_{k_n+j}]| < |f[x_{k_n-1}, \ldots, x_{k_n+j+1}]|$, **then** $k_n := k_n - 1$
  end.

Nonhierarchical stencil selection

For each n, choose k_n such that

$$|f[x_{k_n-1}, \ldots, x_{k_n+M-1}]| = \min_{n-M+1 \le k \le n} |f[x_{k-1}, \ldots, x_{k+M-1}]|.$$

The hierarchical method has the disadvantage that it can produce singularity-crossing stencils for discontinuities in f'' or higher derivatives regardless of M. The nonhierarchical method avoids this problem, but it is biased by $f^{(M)}$ [5, 12]. The hierarchical method is usually preferred; however, for the multiresolution constructions

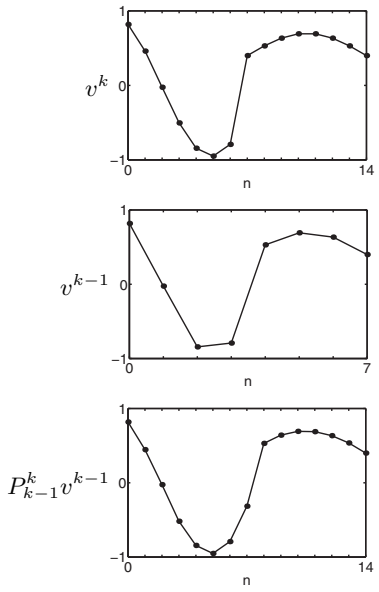

v^k	v^{k-1}	$P^k_{k-1}v^{k-1}$	e^k	d^k
0.8185	0.8185	0.8185	0	
0.4603		0.4460	0.0143	0.0143
−0.0253	−0.0253	−0.0253	0	
−0.5039		−0.5177	0.0138	0.0138
−0.8430	−0.8430	−0.8430	0	
−0.9487		−0.9510	0.0024	0.0024
−0.7916	−0.7916	−0.7916	0	
0.4000		−0.3146	0.7146	0.7146
0.5302	0.5302	0.5302	0	
0.6345		0.6416	−0.0070	−0.0070
0.6925	0.6925	0.6925	0	
0.6925		0.6883	0.0042	0.0042
0.6345	0.6345	0.6345	0	
0.5302		0.5366	−0.0065	−0.0065
0.4000	0.4000	0.4000	0	

FIG. 3.2. *An example of point-value ENO decomposition using cubic ENO interpolation. The largest error* $e^k_7 = 0.7146$ *occurs in the interval containing the discontinuity.*

developed in this paper, the nonhierarchical method is often the better choice. This will be discussed further in section 6.1.

Define $\mathcal{I}^{\mathrm{ENO}}_k : V^k \to \mathcal{F}$ as ENO interpolation. For uniformly spaced x_n, define

$$(P^{\mathrm{ENO}}v)_n = (\mathcal{I}^{\mathrm{ENO}}_k v)(x_n/2).$$

P^{ENO} has the property $\downarrow P^{\mathrm{ENO}} = I$. We call an operator with this property an *interpolatory* operator.

3.2. Point-value discretization. ENO interpolation is the reconstruction operator in point-value ENO multiresolution. Define $\mathcal{D}_k$ as sampling point values:

$$v^k_n = (\mathcal{D}_k f)_n = f(x^k_n), \quad x^k_n = 2^{-k}n.$$

The interpolant $\mathcal{R}_k v^k = \mathcal{I}^{\mathrm{ENO}}_k v^k$ is equal to f at the point-values $f(x^k_n)$, so the consistency relationship $\mathcal{D}_k\mathcal{R}_k = I_{V^k}$ is trivially satisfied. The decimation operator is downsampling, $v^{k-1} = D^k_{k-1}v^k = \downarrow v^k$. The prediction operator $P^k_{k-1} = \mathcal{D}_k\mathcal{R}_{k-1}$ is ENO interpolatory prediction,

$$(P^k_{k-1}v^{k-1})_n = (\mathcal{I}^{\mathrm{ENO}}_k v^{k-1})(x^k_n) = (P^{\mathrm{ENO}}v^{k-1})_n.$$

The prediction error $e^k = v^k - P^k_{k-1}v^{k-1}$ is nonzero only for odd n. For a nonredundant representation, the detail is encoded by keeping samples at odd n; $d^k_n = e^k_{2n+1}$ (see Figure 3.2).

3.3. Cell-average and hat-based discretizations. In most multiresolution schemes, smoothing is applied before downsampling to avoid aliasing in the coarser subbands. The cell-average and hat-based discretizations use local averages to achieve this smoothing. Suppose $f \in L^1_{\mathrm{loc}}$ is discretized by computing weighted averages

$$(\mathcal{D}_k f)_n = \int 2^k \phi(n - 2^k x)\, f(x)\, dx,$$

where ϕ is a compactly supported weighting function. Equivalently, $(\mathcal{D}_k f)_n = (\phi_k * f)(x_n^k)$, with $\phi_k(x) = 2^k\phi(2^k x)$. For cell-average discretization, ϕ is the Haar scaling function

$$\phi(x) = \begin{cases} 1, & 0 \le x < 1, \\ 0, & \text{otherwise.} \end{cases}$$

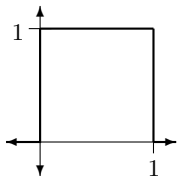

The discretization $(\mathcal{D}_k f)_n$ is the average over the cell $c_n^k = (\,2^{-k}(n-1), 2^{-k}n\,)$,

$$(\mathcal{D}_k f)_n = 2^k \int_{c_n^k} f(x)\,dx,$$

hence the name "cell-average." The dilation equation of the Haar scaling function $\phi(x) = \phi(2x)+\phi(2x-1)$ implies that $v_n^{k-1} = \frac{1}{2}v_{2n}^k + \frac{1}{2}v_{2n-1}^k$. Therefore, the decimation operator is $(D_k^{k-1}v^k)_n = \frac{1}{2}v_{2n}^k + \frac{1}{2}v_{2n-1}^k$.

For hat-based discretization, ϕ is the hat function

$$\phi(x) = \begin{cases} 1+x, & -1 \le x \le 0, \\ 1-x, & 0 \le x \le 1, \\ 0, & \text{otherwise.} \end{cases}$$

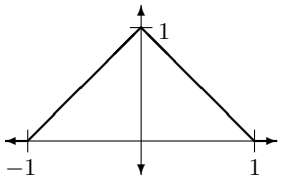

As with cell-average discretization, the dilation equation of ϕ determines D_k^{k-1}:

$$\begin{aligned} \phi(x) &= \tfrac{1}{2}\phi(2x-1) + \phi(2x) + \tfrac{1}{2}\phi(2x+1), \\ (D_k^{k-1}v^k)_n &= \tfrac{1}{4}v_{2n-1}^k + \tfrac{1}{2}v_{2n}^k + \tfrac{1}{4}v_{2n+1}^k. \end{aligned}$$

Consider the reconstruction operators for these discretization operators. To satisfy the consistency requirement $\mathcal{D}_k\mathcal{R}_k = I_{V^k}$, one approach is to modify the point-value ENO interpolation described in section 3.1 such that the reconstruction function attains averages rather than point-values [1].

Harten's approach to constructing $\mathcal{R}_k$ is *reconstruction via primitive function* [6, 14]. The idea is to reduce reconstruction to interpolation (that is, to point-value reconstruction). For cell-average discretization, the relationship between f and its primitive $\mathring{f}$ is

$$\mathring{f}(x) = \int_0^x f(y)\,dy, \qquad f(x) = \frac{d}{dx}\mathring{f}(x).$$

Set $\mathring{v}_{-1}^k = 0$, then the relationship between v^k and $\mathring{v}^k$ is

$$\mathring{v}_n^k = 2^{-k}\sum_{m=0}^{n} v_m^k, \quad v_n^k = 2^k(\mathring{v}_n^k - \mathring{v}_{n-1}^k), \quad n = 0, \dots J_k - 1. \tag{3.3}$$

Let $\mathcal{I}_k$ be any interpolatory operator, for example, ENO interpolation. Define the reconstruction operator as

$$(\mathcal{R}_k v^k)(x) = \frac{d}{dx}\mathcal{I}_k\mathring{v}^k(x). \tag{3.4}$$

This $\mathcal{R}_k$ satisfies the consistency relationship (2.1): For any $v^k \in V^k$,

$$(\mathcal{D}_k \mathcal{R}_k v^k)_n = 2^k \int_{x^k_{n-1}}^{x^k_n} \frac{d}{dx}(\mathcal{I}_k \mathring{v}^k)\, dx = 2^k(\mathring{v}^k_n - \mathring{v}^k_{n-1}) = v^k_n.$$

The derivative in (3.4) should be interpreted in the weak sense. When $\mathcal{I}_k$ is ENO interpolation, $\mathcal{I}_k \mathring{v}^k$ is piecewise differentiable, so $\mathcal{R}_k v^k$ is piecewise continuous.

Using (3.3) to obtain $\mathring{v}^k$ from v^k, the prediction operator $P^k_{k-1} = \mathcal{D}_k \mathcal{R}_{k-1}$ is

$$(P^k_{k-1} v^{k-1})_n = 2^k \left[(\mathcal{I}_{k-1}\mathring{v}^{k-1})(x^k_n) - (\mathcal{I}_{k-1}\mathring{v}^{k-1})(x^k_{n-1})\right]. \tag{3.5}$$

The approach is similar for hat-based discretization. As developed in [6], the relationship between f and its primitive is

$$\mathring{f}(x) = \int_0^x \int_0^y f(z)\, dz\, dy, \qquad f(x) = \frac{d^2}{dx^2}\mathring{f}(x).$$

Setting $\mathring{v}^k_n = 0$ for $n < 0$, there is a bijection between v^k and $\mathring{v}^k$:

$$\mathring{v}^k_n = 4^{-k} \sum_{m=0}^{n} \sum_{j=0}^{m} v^k_j, \quad v^k_n = 4^k(\mathring{v}^k_{n+1} - 2\mathring{v}^k_n + \mathring{v}^k_{n-1}), \quad n = 0, \dots J_k - 1.$$

Define the reconstruction operator analogously to (3.4),

$$(\mathcal{R}_k v^k)(x) = \frac{d^2}{dx^2}\mathcal{I}_k \mathring{v}^k(x). \tag{3.6}$$

The second derivative should be interpreted in the weak sense. While the first derivative in (3.4) can produce jump discontinuities, (3.6) can produce Dirac measures.

It is true that (3.6) satisfies $\mathcal{D}_k \mathcal{R}_k = I_{V^k}$, but verifying this is more cumbersome than in the cell-average case; see [6]. The prediction operator $P^k_{k-1} = \mathcal{D}_k \mathcal{R}_{k-1}$ is

$$\begin{aligned}(P^k_{k-1} v^{k-1})_n = 4^k \big[&(\mathcal{I}_{k-1}\mathring{v}^{k-1})(x^k_{n+1}) \\ &-2(\mathcal{I}_{k-1}\mathring{v}^{k-1})(x^k_n) + (\mathcal{I}_{k-1}\mathring{v}^{k-1})(x^k_{n-1})\big].\end{aligned} \tag{3.7}$$

Detail encoder and decoder operators can be found using the property that $D^{k-1}_k e^k = 0$. For cell-average discretization, this is $e^k_{2n} = -e^k_{2n-1}$; thus a choice of detail encoder and decoder operators is

$$d^k_n = (G_k e^k)_n = e^k_{2n-1}, \qquad \begin{cases} e^k_{2n-1} = (\tilde{G}_k d^k)_{2n-1} = d^k_n, \\ e^k_{2n} = (\tilde{G}_k d^k)_{2n} = -d^k_n. \end{cases}$$

For hat-based discretization, $e^k_{2n} = -\frac{1}{2}(e^k_{2n-1} + e^k_{2n+1})$. As proposed in [6], the detail operators can be

$$d^k_n = (G_k e^k)_n = e^k_{2n-1}, \qquad \begin{cases} e^k_{2n-1} = (\tilde{G}_k d^k)_{2n-1} = d^k_n, \\ e^k_{2n} = (\tilde{G}_k d^k)_{2n} = -\frac{1}{2}(d^k_n + d^k_{n+1}). \end{cases}$$

Cell-average and hat-based discretizations are two members of a family of spline-based discretizations. Denote the order of a spline discretization by N, with cell-average discretization as $N = 1$ and hat-based discretization as $N = 2$. Point-value discretization fits into this classification as $N = 0$.

For general N, the weight function ϕ is the B-spline of order $N-1$, and $\mathring{f}$ is related to f through an Nth-order integral. The next sections develop the construction of the framework operators for a variety of discretizations, including spline-based discretization of any order (section 6.1).

4. Construction with general discretizations. Harten's framework is defined starting with a discretization operator $\mathcal{D}_k$ and a reconstruction operator $\mathcal{R}_k$ in the continuous domain. These operators are then used to define the decimation and prediction operators in the discrete domain. In this section, the reverse is done: Construction begins with the discrete operators.

Through this section, let h be an FIR filter, and define the decimation operator $D_k^{k-1}v^k = \downarrow(h * v^k)$.

4.1. Detail encoding. Considering h as a wavelet lowpass filter, let $\tilde{h}$, g, and $\tilde{g}$ be corresponding dual lowpass, highpass, and dual highpass wavelet filters, and define $H_k v = D_k^{k-1} v$, $G_k v = \downarrow(g * v)$, $\tilde{H}_k v = \tilde{h} *\uparrow v$, $\tilde{G}_k = \tilde{g} *\uparrow v$.

Suppose this wavelet transform is applied to e^k. Since $H_k e^k = D_k^{k-1} e^k = 0$ by (2.4), the lowpass component is zero (see Figure 4.1). Therefore, G_k and $\tilde{G}_k$ from this wavelet transform are a choice of detail operators for nonredundant decomposition.

Since G_k and $\tilde{G}_k$ are linear, the nonredundant decomposition shown in Figure 4.2 is equivalent to a one-stage lifting scheme (see Figure 4.3).

Remark 1. More generally, any linear operators G_k from V^k to V^{k-1} and $\tilde{H}_k$ and $\tilde{G}_k$ from V^{k-1} to V^k satisfying $\tilde{H}_k D_k^{k-1} + \tilde{G}_k G_k = I_{V^k}$ constitute a lifting scheme as shown in Figure 4.3.

To construct the detail operators for a given decimation filter h, a wavelet must be constructed with this same filter h as its lowpass filter. The perfect reconstruction of the wavelet scheme implies the conditions

$$h(z)\,\tilde{h}(z) \;+\; g(z)\,\tilde{g}(z) = 2,$$
$$h(z)\,\tilde{h}(-z) \;+\; g(z)\,\tilde{g}(-z) = 0.$$

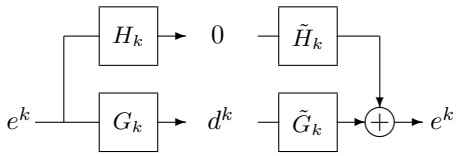

FIG. 4.1. *A wavelet transform of* e^k.

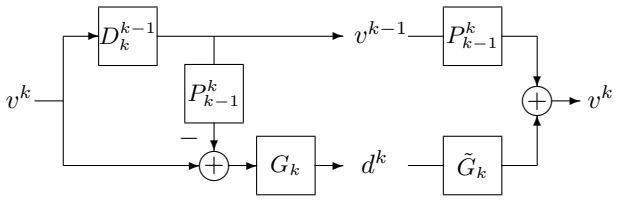

FIG. 4.2. *Nonredundant decomposition using detail encoding.*

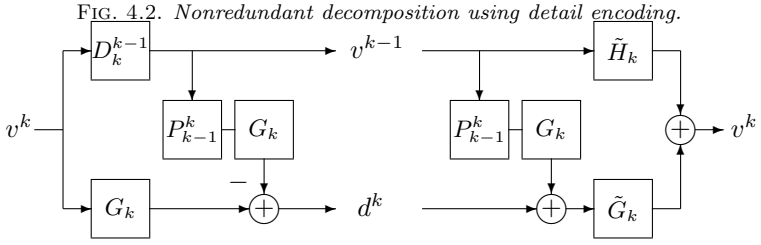

FIG. 4.3. *Nonredundant decomposition as a one-stage lifting scheme.*

If $g(z) = z^{-1}\,\tilde{h}(-z)$ and $\tilde{g}(z) = z\,h(-z)$, the second condition is satisfied. The first condition then reduces to $h(z)\,\tilde{h}(z) + h(-z)\,\tilde{h}(-z) = 2$, which is true if $(h * \tilde{h})_0 = 1$ and $(h * \tilde{h})_n = 0$ for nonzero even n. Thus $\tilde{h}$ must satisfy the linear system

$$\sum_j \tilde{h}_j\, h_{2n-j} = \begin{cases} 1 & \text{if } n = 0, \\ 0 & \text{if } n \neq 0 \end{cases} \qquad \text{for all } n. \tag{4.1}$$

For example, consider $h(z) = az^2 + bz + c + dz^{-1} + ez^{-2}$. If $\tilde{h}$ is assumed to have the form $\tilde{h}(z) = \tilde{h}_{-1}\,z + \tilde{h}_0 + \tilde{h}_1\,z^{-1}$, (4.1) becomes the matrix equation

$$\begin{bmatrix} b & a & 0 \\ d & c & b \\ 0 & e & d \end{bmatrix} \begin{bmatrix} \tilde{h}_{-1} \\ \tilde{h}_0 \\ \tilde{h}_1 \end{bmatrix} = \begin{bmatrix} 0 \\ 1 \\ 0 \end{bmatrix}.$$

Provided a nonzero determinant $\kappa = bcd - ad^2 - b^2e \neq 0$, the solution is $\tilde{h}(z) = \frac{1}{\kappa}(-adz + bd - bez^{-1})$ and

$$\begin{aligned} h(z) &= az^2 + bz + c + dz^{-1} + ez^{-2}, \quad & g(z) &= \frac{1}{\kappa}\left(ad + bdz^{-1} + bez^{-2}\right), \\ \tilde{h}(z) &= \frac{1}{\kappa}\left(-adz + bd - bez^{-1}\right), & \tilde{g}(z) &= az^3 - bz^2 + cz - d + ez^{-1}. \end{aligned} \tag{4.2}$$

It is also possible to select filters from existing wavelet families. Given a number of reconstruction vanishing moments N and decomposition vanishing moments $\tilde{N}$ where $N + \tilde{N}$ is even, the spline wavelet filters are

$$h(z) = z^{\lfloor N/2 \rfloor} \left(\frac{1 + z^{-1}}{2}\right)^N, \tag{4.3}$$

$$\tilde{h}(z) = 2z^{\lceil \tilde{N}/2 \rceil} \left(\frac{1 + z^{-1}}{2}\right)^{\tilde{N}} \sum_{n=0}^{M} \binom{M+n}{n} (-4)^{-n} (z - 2 + z^{-1})^n, \tag{4.4}$$

where $M = \frac{1}{2}(N + \tilde{N}) - 1$, $\lfloor \cdot \rfloor$ denotes the floor function, and $\lceil \cdot \rceil$ denotes the ceiling function [11]. The corresponding highpass filters are $g(z) = \frac{1}{2}z^{-1}\tilde{h}(-z)$ and $\tilde{g}(z) = 2zh(-z)$. The lowpass filter h is the decimation filter corresponding to the spline discretization of order N. If the prediction operator can predict locally polynomial signals, then vanishing moments in g are unnecessary, and $\tilde{N}$ should be 0 (or 1, if N is odd) to minimize the support of g.

Setting $N = 2$, $\tilde{N} = 0$ yields the hat filters

$$h(z) = z\left(\frac{1 + z^{-1}}{2}\right)^2 = \tfrac{1}{4}z + \tfrac{1}{2} + \tfrac{1}{4}z^{-1}, \qquad g(z) = z^{-1},$$

$$\tilde{h}(z) = 2\sum_{n=0}^{0} (-4)^{-n}(z - 2 + z^{-1})^n = 2, \qquad \tilde{g}(z) = -\tfrac{1}{2}z^2 + z - \tfrac{1}{2}.$$

These lead to the same encoding and decoding operators as before in section 3.3:

$$\begin{aligned} &\textit{Encoding} \qquad d^k = {\downarrow}(e^k * g) \quad \Leftrightarrow \quad d^k_n = e^k_{2n-1}, \\ &\textit{Decoding} \qquad e^k = ({\uparrow}\, d^k) * \tilde{g} \quad \Leftrightarrow \quad \begin{cases} e^k_{2n-1} = d^k_n, \\ e^k_{2n} = -\frac{1}{2}(d^k_n + d^k_{n+1}). \end{cases} \end{aligned}$$

Section 6.1 will expand upon this example to construct spline schemes for $N > 2$.

Remark 2. If h, $\tilde{h}$, g, and $\tilde{g}$ satisfy the perfect reconstruction conditions, then so do the scaled and shifted filters

$$h'(z) = \alpha z^{2j} h(z), \qquad g'(z) = \beta z^{2k} g(z),$$
$$\tilde{h}'(z) = \frac{1}{\alpha} z^{-2j} \tilde{h}(z), \qquad \tilde{g}'(z) = \frac{1}{\beta} z^{-2k} \tilde{g}(z).$$

Notice that the detail encoding and decoding operators are not uniquely determined by h. Consider the filter $h(z) = \frac{1}{8}z + \frac{3}{8} + \frac{3}{8}z^{-1} + \frac{1}{8}z^{-2}$. With the spline wavelet approach with $N = 3$ and $\tilde{N} = 1$, the filters g and $\tilde{g}$ are

$$g(z) = \tfrac{1}{4}z + \tfrac{3}{4} - \tfrac{3}{4}z^{-1} - \tfrac{1}{4}z^{-2}, \qquad \tilde{g}(z) = \tfrac{1}{4}z^2 - \tfrac{3}{4}z + \tfrac{3}{4} - \tfrac{1}{4}z^{-1}.$$

Using (4.2), the filters are

$$g(z) = 3z^{-1} + z^{-2}, \qquad \tilde{g}(z) = -\tfrac{1}{8}z^2 + \tfrac{3}{8}z - \tfrac{3}{8} + \tfrac{1}{8}z^{-1}.$$

There is a lot of flexibility in designing the detail operators. Harten's framework does not even require that they are linear, only that $\tilde{G}_k G_k e^k = e^k$ for all $e^k \in \mathcal{N}(D_k^{k-1})$.

4.2. Diagonalizing the decimation operator. Following the "via primitive" technique (section 3.3), our next step is to choose maps under which D_k^{k-1} becomes pure downsampling.

THEOREM 4.1. *Suppose $D_k^{k-1} : V^k \to V^{k-1}$ is any linear and surjective operator, then there exists bijections T_k on V^k and $\tilde{T}_{k-1}$ on V^{k-1} such that*

$$\tilde{T}_{k-1}^{-1} D_k^{k-1} T_k = \downarrow . \tag{4.5}$$

For any such maps $\tilde{T}_{k-1}$ and T_k, P_{k-1}^k is a consistent prediction operator if and only if $T_k^{-1} P_{k-1}^k \tilde{T}_{k-1}$ is an interpolatory operator.

Proof. One way to construct T_k and $\tilde{T}_{k-1}$ is to interpret D_k^{k-1} as a $J_{k-1} \times J_k$ matrix, and let $D_k^{k-1} = U\Sigma V^*$ be a singular value decomposition (SVD). Since D_k^{k-1} is surjective, the singular values $\sigma_1, \ldots, \sigma_{J_{k-1}}$ are all positive. Let S be the $J_{k-1} \times J_{k-1}$ diagonal matrix $S_{ii} = \sigma_i$, and let P be the $J_k \times J_k$ permutation matrix such that $S^{-1}\Sigma P = \left[I \,\middle|\, 0 \right] P = \downarrow$. Then

$$D_k^{k-1} \;=\; US(S^{-1}\Sigma P)P^* V^* = US \downarrow (VP)^*.$$

So a choice for the maps is $T_k = VP$ and $\tilde{T}_{k-1} = US$.

For any interpolatory operator Q_{k-1}^k, the prediction operator

$$P_{k-1}^k = T_k Q_{k-1}^k \tilde{T}_{k-1}^{-1} \tag{4.6}$$

is consistent: $D_{k-1}^k T_k Q_{k-1}^k \tilde{T}_{k-1}^{-1} = \tilde{T}_{k-1} \downarrow Q_{k-1}^k \tilde{T}_{k-1}^{-1} = I_{V^{k-1}}$. Conversely, if P_{k-1}^k is consistent, $\downarrow T_k^{-1} P_{k-1}^k \tilde{T}_{k-1} = \tilde{T}_{k-1}^{-1} D_k^{k-1} P_{k-1}^k \tilde{T}_{k-1} = I_{V^{k-1}}$. Thus P_{k-1}^k is a consistent prediction operator if and only if $T_k^{-1} P_{k-1}^k \tilde{T}_{k-1}$ is interpolatory. ∎

Remark 3. Furthermore, if an SVD of D_k^{k-1} is available, then $E_k v = [0 | I_{J_{k-1} \times J_{k-1}}] V^* v$, and $F_k d = E_k^* d$ are valid detail operators.

Given $\tilde{H}_k$, G_k, and $\tilde{G}_k$ such that $\tilde{H}_k D_k^{k-1} + \tilde{G}_k G_k = I_{V^k}$, a practical choice for the diagonalization maps is

$$T_k = \left[\tilde{H}_k \; \tilde{G}_k \right] P^*, \qquad \tilde{T}_{k-1} = I_{V^{k-1}}, \tag{4.7}$$

where P is the permutation matrix in the proof of Theorem 4.1. Then prediction takes the form $P_{k-1}^k v^{k-1} = \tilde{H}_k v^{k-1} + \tilde{G}_k w$, where w may be any element of V^{k-1}.

Moreover, (4.7) yields a strategy for correcting the consistency of a nonconsistent prediction operator. Let $\hat{P}_{k-1}^k : V^{k-1} \to V^k$ be any operator, then

$$P_{k-1}^k v^{k-1} = \tilde{H}_k v^{k-1} + \tilde{G}_k G_k \hat{P}_{k-1}^k v^{k-1} \tag{4.8}$$

is consistent and if $\hat{P}_{k-1}^k$ is already consistent, then $P_{k-1}^k = \hat{P}_{k-1}^k$. Such a prediction operator may be efficiently implemented in lifting scheme form as in Figure 4.3:

$$\textit{Encoding} \begin{cases} v^{k-1} = D_k^{k-1} v^k, \\ d^k = G_k v^k - G_k \hat{P}_{k-1}^k v^{k-1}, \end{cases} \qquad \textit{Decoding} \begin{cases} \tilde{d}^k = d^k + G_k \hat{P}_{k-1}^k v^{k-1}, \\ v^k = \tilde{H}_k v^{k-1} + \tilde{G}_k \tilde{d}^k. \end{cases}$$

The maps T_k and $\tilde{T}_{k-1}$ diagonalize D_k^{k-1} to the operation of pure downsampling. In the cell-average and hat-based constructions, these maps are seen as a relationship between the original signal v^{k-1} and its primitive $\mathring{v}^{k-1}$:

$$v^{k-1} \xrightarrow{\tilde{T}_{k-1}^{-1}} \mathring{v}^{k-1}, \qquad \mathring{v}^k \xrightarrow{T_k} v^k.$$

At least for spline discretizations, there are diagonalization maps such that $\tilde{T}_k = T_k$. However, $\tilde{T}_k$ and T_k need not be equal in general.

4.3. Prediction for convolution-based decimation. The preceding discussion applies to constructions with any linear and surjective D_{k-1}^k. In the rest of our construction we restrict to decimation of the form $D_{k-1}^k v^k = \downarrow(h * v^k)$, where h is an FIR filter.

In both the cell-average and hat-based constructions, the relationship between v^k and $\mathring{v}^k$ is linear shift-invariant, which suggests diagonalization maps of the form

$$T_k \mathring{v}^k = a * \mathring{v}^k, \quad \tilde{T}_{k-1}^{-1} v^{k-1} = b * v^{k-1}.$$

Moreover, from a design point of view, this is a convenient choice of maps since if Q_{k-1}^k is shift-invariant, then so is P_{k-1}^k.

Ignoring boundary issues for the moment, consider the scheme on the infinite grid. Discrete consistency $D_k^{k-1} P_{k-1}^k = I_{V^{k-1}}$ can be written using (1.2) as

$$\tfrac{1}{2}\left[h(z)\mathcal{Z}\{P_{k-1}^k v^{k-1}\}(z) + h(-z)\mathcal{Z}\{P_{k-1}^k v^{k-1}\}(-z)\right] = v^{k-1}(z^2).$$

Consider $P_{k-1}^k v^{k-1} = a * Q_{k-1}^k (b * v^{k-1})$, with $a(z) = h(-z)$. Then

$$\begin{aligned} \tfrac{1}{2}\left[h(z)h(-z)\mathcal{Z}\{Q_{k-1}^k(b * v^{k-1})\}(z) + h(-z)h(z)\mathcal{Z}\{Q_{k-1}^k(b * v^{k-1})\}(-z)\right] &= v^{k-1}(z^2) \\ h(z)h(-z)\tfrac{1}{2}\left[\mathcal{Z}\{Q_{k-1}^k(b * v^{k-1})\}(z) + \mathcal{Z}\{Q_{k-1}^k(b * v^{k-1})\}(-z)\right] &= v^{k-1}(z^2). \end{aligned}$$

Let $\mathring{v}^{k-1} = b * v^{k-1}$, then since Q_{k-1}^k is interpolatory,

$$\tfrac{1}{2}\left[\mathcal{Z}\{Q_{k-1}^k \mathring{v}^{k-1}\}(z) + \mathcal{Z}\{Q_{k-1}^k \mathring{v}^{k-1}\}(-z)\right] = \mathcal{Z}\{\uparrow\downarrow(Q_{k-1}^k \mathring{v}^{k-1})\}(z) = \mathring{v}^{k-1}(z^2).$$

Thus

$$h(z)h(-z)\left[b(z^2)v^{k-1}(z^2)\right] = v^{k-1}(z^2) \quad \Rightarrow \quad b(z^2) = \frac{1}{h(z)h(-z)}.$$

Since $h(z)h(-z)$ is even, $b(z)$ is well defined by this expression. Therefore, for any interpolatory operator Q^k_{k-1},

$$P^k_{k-1}v^{k-1} = a * Q^k_{k-1}(b * v^{k-1}) \tag{4.9}$$

is a consistent prediction operator with

$$a(z) = h(-z), \quad b(z^2) = \frac{1}{h(z)h(-z)}.$$

For finite-length signals, the consistency of the prediction operator (4.9) does not hold near the boundaries. The boundaries can be corrected using (4.8).

Remark 4. If c satisfies $c(z) = c(-z)$, the prediction operator $P^k_{k-1}v^{k-1} = a * Q^k_{k-1}(b * v^{k-1})$ with filters

$$b(z^2) = \frac{1}{c(z)h(z)h(-z)}, \qquad a(z) = c(z)h(-z)$$

is also consistent. In particular, b and a may be rescaled with $c(z) = \kappa$.

Beware that b is typically an unstable filter. If $h(z)$ has a zero at r, then $b(z)$ has a pole at r^2. Depending on the rate of unstable growth and the signal length, a direct implementation of (4.9) may yet be numerically tractable. Otherwise, (4.9) should be considered conceptually and then implemented using other diagonalization maps (for example, (4.7)).

This construction reproduces the cell-average and hat-based discretization strategies in section 3.3. Let $\mathcal{I}_k$ be an interpolatory operator, and define Q^k_{k-1} by $(Q^k_{k-1}v^{k-1})_n = (\mathcal{I}_{k-1}v^{k-1})(x^k_n)$. If h is the cell-average decimation filter $h(z) = \frac{1}{2} + \frac{1}{2}z^{-1}$ and $\kappa = 2^{k+1}$,

$$\begin{aligned} b(z^2) = \frac{1}{\kappa\, h(z)h(-z)} \;&=\; \frac{2^{1-k}}{1-z^{-2}} \qquad \Rightarrow \qquad b(z) \;=\; \frac{2^{1-k}}{1-z^{-1}}, \\ a(z) = \kappa\, h(-z) &= 2^k(1-z^{-1}). \end{aligned}$$

Convolution with b is cumulative summation, and convolution with a is backward differencing. Define

$$\tilde{v}^{k-1}_n = (b * v^{k-1})_n = 2^{1-k}\sum_{m=1}^{n} v^{k-1}_m,$$

then the prediction operator is

$$\begin{aligned} (P^k_{k-1}v^{k-1})_n = (a * Q^k_{k-1}\tilde{v}^{k-1})_n &= 2^k\left[(Q^k_{k-1}\tilde{v}^{k-1})_n - (Q^k_{k-1}\tilde{v}^{k-1})_{n-1}\right] \\ &= 2^k\left[(\mathcal{I}_{k-1}\tilde{v}^{k-1})(x^k_n) - (\mathcal{I}_{k-1}\tilde{v}^{k-1})(x^k_{n-1})\right]. \end{aligned}$$

Compare this to the cell-average prediction described in section 3.3, which is

$$(P^k_{k-1}v^{k-1})_n = 2^k\left[(\mathcal{I}_{k-1}\mathring{v}^{k-1})(x^k_n) - (\mathcal{I}_{k-1}\mathring{v}^{k-1})(x^k_{n-1})\right], \quad \mathring{v}^{k-1}_n = 2^{1-k}\sum_{m=1}^{n} v^{k-1}_m.$$

Notice that $\tilde{v}^{k-1} = b*v^{k-1}$ has the same role as the primitive samples $\mathring{v}^{k-1}_n = \mathring{f}(x^{k-1}_n)$. Section 4.4 generalizes the notion of primitive through this connection.

For the hat-based prediction as in section 3.3, set $h(z) = \frac{1}{4}z + \frac{1}{2} + \frac{1}{4}z^{-1}$ and $\kappa = -4^{k+1}$:

$$b(z^2) = \frac{1}{\kappa\, h(z)h(-z)} = \frac{4^{1-k}z^{-2}}{(1-z^{-2})^2} \qquad \Rightarrow \qquad b(z) = \frac{4^{1-k}z^{-1}}{(1-z^{-1})^2},$$
$$a(z) = \kappa\, h(-z) = 4^k(z - 2 + z^{-1}).$$

The interpolatory operator Q^k_{k-1} must be sufficiently regular to compensate for applying the highpass filter a. For hat-based prediction, $a * Q^k_{k-1}\mathring{v}^{k-1}$ is the second difference of $Q^k_{k-1}\mathring{v}^{k-1}$, which has Dirac measures if Q^k_{k-1} is not smooth. One way to make a smoother version of Q^k_{k-1} is by defining

$$\tilde{Q}^k_{k-1}\mathring{v}^{k-1} = \operatorname*{arg\,min}_{q:\downarrow q = \mathring{v}^{k-1}} \left\|Q^k_{k-1}\mathring{v}^{k-1} - q\right\|_2^2 + \|\lambda \cdot (d * q)\|_2^2, \tag{4.10}$$

where d is a finite difference filter and λ_n weights the amount of regularization around point n. The minimization is equivalent to solving a sparse linear system.

Remark 5. There is no restriction that a prediction must be formulated in the same way for all scales k. The filters a and b may depend on k.

4.4. Operators $\mathcal{D}_k$ and $\mathcal{R}_k$. Knowing only the discrete operators D^{k-1}_k, P^k_{k-1}, G_k, and $\tilde{G}_k$ is sufficient for implementation. However, to complete Harten's framework, this section finds operators $\mathcal{D}_k$ and $\mathcal{R}_k$ consistent with the discrete operators. In this section, complications at the boundaries are ignored by working on the infinite grid.

Given a discrete signal g, define its delta sequence at resolution level k as

$$g_{\delta_k}(x) \stackrel{\text{def}}{=} \sum_{n\in\mathbb{Z}} g_n\, \delta(x - x^k_n), \quad x^k_n = 2^{-k}n.$$

Suppose that $h(z)$ has at least one root at $z = -1$ and is normalized as $h(1) = 1$. Analogous to the scaling function in wavelet theory, define

$$\phi(x) = 2\sum_n h_n\, \phi(2x - n). \tag{4.11}$$

This determines $\hat{\phi}$ up to a scale factor [17], which is chosen such that $\hat{\phi}(0) = 1$. Define the discretization operator

$$(\mathcal{D}_k f)_n = (\phi_k * f)(x^k_n), \qquad \phi_k(x) = 2^k\phi(2^k x). \tag{4.12}$$

Now consider the reconstruction operator $\mathcal{R}_k$. Let $\mathcal{I}_k$ be any interpolatory operator. Define the corresponding interpolatory operator $(Q^k_{k-1}v^{k-1})_n = (\mathcal{I}_{k-1}v^{k-1})(x^k_n)$. Section 4.3 defines the prediction operator as

$$\begin{aligned}(P^k_{k-1}v^{k-1})_n &= \big(a * Q^k_{k-1}(b * v^{k-1})\big)_n \\ &= \big(a_{\delta_k} * \mathcal{I}_{k-1}(b * v^{k-1})\big)(x^k_n),\end{aligned} \tag{4.13}$$

where $b(z^2) = 1/\big(h(z)h(-z)\big)$ and $a(z) = h(-z)$. Suppose that the reconstruction operator has the form $\mathcal{R}_k v^k = \xi_k * \mathcal{I}_k(b * v^k)$, where ξ_k is a distribution. Then the prediction operator is defined by the framework to be

$$\begin{aligned}(P^k_{k-1}v^{k-1})_n &= (\mathcal{D}_k\mathcal{R}_{k-1}v^{k-1})_n \\ &= \big(\phi_k * \xi_{k-1} * \mathcal{I}_{k-1}(p * v^{k-1})\big)(x^k_n).\end{aligned}$$

In order to agree with the construction of P_{k-1}^k in (4.13), ξ_{k-1} is defined implicitly by $\phi_k * \xi_{k-1} = a_{\delta_k}$. Since h is FIR, ϕ_k has a finite degree of continuity, and hence $\left|\hat{\xi}_{k-1}(\omega)\right| = |\hat{a}_{\delta_k}(\omega)| / |\hat{\phi}_k(\omega)| \le \|a\|_{\ell^1} / |\hat{\phi}_k(\omega)| = O(|\omega|^p)$ for some finite p. Therefore, ξ_{k-1} is a tempered distribution.

Let $w(z) = 1/b(z)$, then since $w = \downarrow(h * a)$ and $\phi_{k-1} = h_{\delta_k} * \phi_k$,

$$\phi_k * \xi_{k-1} = a_{\delta_k} \quad \Rightarrow \quad h_{\delta_k} * \phi_k * \xi_{k-1} = (h * a)_{\delta_k} \quad \Rightarrow \quad \phi_{k-1} * \xi_{k-1} = w_{\delta_{k-1}}.$$

So ξ_k is also given by $\phi_k * \xi_k = w_{\delta_k}$. Define the reconstruction operator as

$$\mathcal{R}_k v^k = \xi_k * \mathcal{I}_k(b * v^k), \qquad \phi_k * \xi_{k-1} = a_{\delta_k}. \tag{4.14}$$

For example, in the cell-average case, $\mathcal{R}_k$ should be $\mathcal{R}_k v^k = \frac{d}{dx}\mathcal{I}_k(b * v^k)$, with $b(z) = 2^{-k}(1 - z^{-1})^{-1}$ and $\xi_k = -\delta'$ (such that $\xi_k * (\cdot) = \frac{d}{dx}(\cdot)$).

This approach to the reconstruction operator provides a general notion of primitive. If the primitive samples are $\mathring{v}^k = b * v^k$, then

$$\begin{aligned} \mathring{f}^k(x_n^k) = \mathring{v}_n^k = (b * v^k)_n = (b_{\delta_k} * \phi_k * f)(x_n^k), \\ (\xi_k * \mathring{f}^k)(x_n^k) = (\xi_k * b_{\delta_k} * \phi_k * f)(x_n^k) = (b_{\delta_k} * w_{\delta_k} * f)(x_n^k) = f(x_n^k), \end{aligned}$$

which suggests defining a "generalized primitive" $\mathring{f}^k$ (see Figure 4.4) by

$$\mathring{f}^k = b_{\delta_k} * \phi_k * f, \qquad f = \xi_k * \mathring{f}^k.$$

In contrast to the primitive in the cell-average and hat-based formulations (section 3.3), the generalized primitive $\mathring{f}^k$ is a different function for each scale k. However, for spline discretizations, section 6.1 will show that there is a single primitive independent of k.

THEOREM 4.2. *The discretization and reconstruction operators defined in* (4.12) *and* (4.14) *satisfy the consistency relationship, and* $(\mathcal{D}_k)$ *is nested. Furthermore, the decimation operator* $D_k^{k-1} = \mathcal{D}_{k-1}\mathcal{R}_k$ *and the prediction operator* $P_{k-1}^k = \mathcal{D}_k\mathcal{R}_{k-1}$ *are*

$$D_k^{k-1} v^k = \downarrow(h * v^k), \qquad P_{k-1}^k v^{k-1} = a * Q_{k-1}^k(b * v^{k-1}),$$

where $(Q_{k-1}^k v^{k-1})_n = (\mathcal{I}_{k-1} v^{k-1})(x_n^k)$.

Proof. For any v^k, $(\mathcal{D}_k\mathcal{R}_k v^k)_n = (\phi_k * \xi_k * \mathcal{I}_k \mathring{v}^k)(x_n^k) = (w_{\delta_k} * \mathcal{I}_k \mathring{v}^k)(x_n^k)$. Because $\mathcal{I}_k$ is an interpolatory operator, $(\mathcal{I}_k \mathring{v}^k)(x_n^k) = \mathring{v}_n^k$. Also noting that w_{δ_k} is a delta sequence, the convolution is equivalently written as the discrete convolution $(w * \mathring{v}^k)_n$. Thus,

$$(\mathcal{D}_k\mathcal{R}_k v^k)_n \;=\; (w * \mathring{v}^k)_n \;=\; v_n^k.$$

So the consistency relationship is satisfied. Because $\phi_{k-1} = h_{\delta_k} * \phi_k$,

$$v_n^{k-1} \;=\; (\phi_{k-1} * f)(x_n^{k-1}) \;=\; (h_{\delta_k} * \phi_k * f)(x_{2n}^k) \;=\; \downarrow(h * v^k)_n.$$

If $\mathcal{D}_k f = v^k = 0$, then $\mathcal{D}_{k-1} f = v^{k-1} = \downarrow(h * v^k) = 0$. Therefore, $(\mathcal{D}_k)$ is nested. Furthermore, consistency and nestedness imply that

$$D_k^{k-1} v^k \;=\; \mathcal{D}_{k-1}\mathcal{R}_k\mathcal{D}_k f \;=\; \mathcal{D}_{k-1} f \;=\; v^{k-1} \;=\; \downarrow(h * v^k).$$

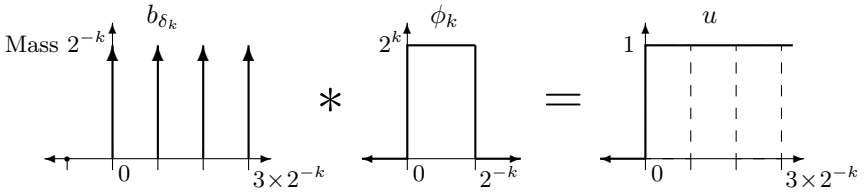

FIG. 4.4. *The cell-average primitive $\mathring{f}$ is related to f by convolution with the unit step $\mathring{f} = b_{\delta_k} * \phi_k * f = u * f$.*

The prediction operator is

$$\begin{aligned}(\mathcal{D}_k \mathcal{R}_{k-1} v^{k-1})_n &= (\phi_k * \xi_{k-1} * \mathcal{I}_{k-1} \mathring{v}^{k-1})(x_n^k) \\ &= \big(a_{\delta_k} * \mathcal{I}_{k-1}(b * v^{k-1})\big)(x_n^k) \\ &= \big(a * Q_{k-1}^k (b * v^{k-1})\big)_n. \qquad \square\end{aligned}$$

Remark 6. If c satisfies $c(z) = c(-z)$, Theorem 4.2 also holds for filters

$$b(z^2) = \frac{1}{c(z)h(z)h(-z)}, \qquad a(z) = c(z)h(-z).$$

Remark 7. Suppose that the interpolation $\mathcal{I}_k$ is linear, shift-invariant, and scale-independent, then

$$(\mathcal{I}_k \mathring{v}^k)(x) = \sum_n 2^k \theta(2^k x - n)\, \mathring{v}_n^k = (\theta_k * \mathring{v}_{\delta_k}^k)(x), \qquad \theta_k(x) = 2^k \theta(2^k x),$$

where the associated function θ satisfies $\theta(0) = 1$ and $\theta(n) = 0$ for all nonzero integers $n \in \mathbb{Z}\backslash\{0\}$. The reconstruction operator becomes $\mathcal{R}_k v^k = \xi_k * \theta_k * b_{\delta_k} * v_{\delta_k}^k$. Let $\tilde{\phi}_k = \xi_k * \theta_k * b_{\delta_k}$ such that $\mathcal{R}_k v^k = \tilde{\phi}_k * v^k$. Since $\phi_k * \xi_k = w_{\delta_k}$ and $w(z) = 1/b(z)$,

$$\phi_k * \tilde{\phi}_k = (\phi_k * \xi_k) * \theta_k * b_{\delta_k} = (w_{\delta_k} * b_{\delta_k}) * \theta_k = \theta_k,$$

so $\tilde{\phi}_k$ satisfies $\phi_k * \tilde{\phi}_k = \theta_k$. Reconstruction reduces to the wavelet reconstruction

$$(\mathcal{R}_k v^k)(x) = \sum_n 2^k \tilde{\phi}(2^k x - n)\, v_n^k,$$

where the dual scaling function $\tilde{\phi}$ satisfies $\phi * \tilde{\phi} = \theta$.

As an example of Theorem 4.2, consider a cell-average ENO with $h(z) = (1+z^{-1})$. Then if $\kappa = 2^k$, $a(z) = 2^{k-1}(1 - z^{-1})$ and $b(z) = 2^{-k}(1 - z^{-1})^{-1}$. The discretization operator is

$$(\mathcal{D}_k f)_n = (\phi_k * f)(x_n^k) = \int_{x_{n-1}^k}^{x_n^k} f(x)\, dx, \qquad \phi(x) = \begin{cases} 1 & \text{if } 0 \le x < 1, \\ 0 & \text{otherwise.} \end{cases}$$

The primitive $\mathring{f}$ is related to f by

$$\mathring{f}(x) = (b_{\delta_k} * \phi_k * f)(x) = (u * f)(x) = \int_0^x f(y)\, dy.$$

Since $\phi_{k+1} * \xi_k = a_{\delta_{k+1}}$,

$$\hat{\xi}_k(\omega) \;=\; \frac{\hat{a}_{\delta_{k+1}}(\omega)}{\hat{\phi}_{k+1}(\omega)} \;=\; \frac{1-\exp(-i\omega 2^{-k-1})}{\frac{1}{i\omega}\left(1-\exp(-i\omega 2^{-k-1})\right)} \;=\; i\omega.$$

That is, convolution with ξ_k is differentiation. Consistent with (3.4) in section 3.3, the reconstruction operator is $(\mathcal{R}_k v^k)(x) = (\xi_k * \mathcal{I}_k \mathring{v}^k)(x) = \frac{d}{dx}(\mathcal{I}_k \mathring{v}^k)(x)$, where $\mathring{v}^k_n = (b * v^k)_n = \mathring{f}(x^k_n)$.

5. Error control. An application of multiresolution decompositions is signal approximation. When the multiresolution transform is linear and orthogonal (or nearly orthogonal), an effective strategy is retaining the M largest transform coefficients and setting the rest to zero. This "M-term approximation" works, since the ℓ^2 error incurred by truncating a coefficient is proportional to its magnitude. However, for nonorthogonal or nonlinear schemes, another strategy is necessary.

Rather than fixing the number of nonzero coefficients, Harten proposed [13] a modified encoding procedure that produces a sparse representation $\hat{m}$ with approximation error less than a specified maximum error.

Define the (hard) thresholding operator

$$\mathrm{tr}(x,\epsilon) = \begin{cases} 0 & \text{if } |x| \le \epsilon, \\ x & \text{if } |x| > \epsilon. \end{cases}$$

Given v^L and a sequence of tolerances (ϵ_k), the modified encoding algorithm is

(5.1)
$$\begin{aligned}
&\textbf{for } k = L, \ldots, 1 \\
&\quad v^{k-1} = D^k_{k-1} v^k \\
&\textbf{end} \\
&\hat{v}^0 = v^0 \\
&\textbf{for } k = 1, \ldots, L \\
&\quad \tilde{d}^k = G_k(v^k - P^k_{k-1}\hat{v}^{k-1}) \\
&\quad \hat{d}^k = \mathrm{tr}(\tilde{d}^k, \epsilon_k) \\
&\quad \hat{v}^k = P^k_{k-1}\hat{v}^{k-1} + \tilde{G}_k \hat{d}^k \\
&\textbf{end} \\
&\hat{m} = (\hat{v}^0, \hat{d}^1, \ldots, \hat{d}^L).
\end{aligned}$$

The thresholds (ϵ_k) control the error of the approximation. Larger values of ϵ_k lead to sparser decompositions, but also larger error. Given a tolerance ϵ, thresholds (ϵ_k) can be selected such that the error is bounded:

$$J_L^{-1/p} \left\| v^L - \hat{v}^L \right\|_p \le \epsilon,$$

where J_k is the length of v^k and $\|\cdot\|_p$ denotes the usual ℓ^p norm.

Such error control has been developed for point-value, cell-average, and hat-based discretizations with zero-padded boundary handling [5, 6]. For point-value discretization, if $\epsilon_k = \epsilon$, then

$$J_L^{-1/p} \left\| v^L - \hat{v}^L \right\|_p \le \epsilon \qquad \text{for } p = 1, 2, \infty. \tag{5.2}$$

For cell-average discretization, if $\epsilon_k = \epsilon\, q^{L-k}$ with $0 < q < 1$, then

$$J_L^{-1/p} \left\| v^L - \hat{v}^L \right\|_p \le \begin{cases} \dfrac{\epsilon}{1-q} & \text{for } p = 1, \infty, \\ \dfrac{\epsilon}{\sqrt{1-q^2}} & \text{for } p = 2. \end{cases} \tag{5.3}$$

For hat-based discretization, if $\epsilon_k = \epsilon\, q^{L-k}$ with $0 < q \le \frac{1}{2}$, then

$$J_L^{-1/p} \left\| v^L - \hat{v}^L \right\|_p \le \begin{cases} \dfrac{\epsilon}{1-2q} & \text{if } 0 < q < \frac{1}{2}, \\ L\epsilon & \text{if } q = \frac{1}{2}, \end{cases} \qquad \text{for } p = 1, 2, \infty. \tag{5.4}$$

See [5, 6] for proofs. Theorem 5.1 provides error control for general discretizations.

THEOREM 5.1. *Let D_k^{k-1} and G_k be linear operators from V^k to V^{k-1}, and $\tilde{H}_k$ and $\tilde{G}_k$ be linear operators from V^{k-1} to V^k satisfying $\tilde{H}_k D_k^{k-1} + \tilde{G}_k G_k = I_{V^k}$, and let P_{k-1}^k be any operator from V^{k-1} to V^k satisfying $D_k^{k-1} P_{k-1}^k = I^{V_{k-1}}$.*

Let $\|\cdot\|$ be a norm, and let α, β be such that

$$\|\tilde{H}_k v\| \le \alpha \|v\| \quad \text{and} \quad \|\tilde{G}_k v\| \le \beta \|v\|_\infty \qquad \text{for all } v \in V^{k-1}, k \le L.$$

If the thresholds (ϵ_k) in the modified encoding algorithm (5.1) satisfy $\epsilon_k = \epsilon\, q^{L-k}$ for some $q \in (0, \alpha^{-1})$, then the reconstruction error is bounded:

$$\left\| v^L - \hat{v}^L \right\| \;<\; \frac{\beta\epsilon}{1-\alpha q}.$$

Proof. First, observe that

$$v^k - \hat{v}^k = (P_{k-1}^k v^{k-1} - P_{k-1}^k \hat{v}^{k-1}) + \tilde{G}_k (d^k - \hat{d}^k).$$

The detail term expands to $d^k - \hat{d}^k = (d^k - \tilde{d}^k) + (\tilde{d}^k - \hat{d}^k) = -G_k(P_{k-1}^k v^k - P_{k-1}^k \hat{v}^{k-1}) + (\tilde{d}^k - \hat{d}^k)$. Therefore,

$$\begin{aligned} v^k - \hat{v}^k &= (I_{V^k} - \tilde{G}_k G_k)(P_{k-1}^k v^{k-1} - P_{k-1}^k \hat{v}^{k-1}) + \tilde{G}_k(\tilde{d}^k - \hat{d}^k) \\ &= \tilde{H}_k D_k^{k-1}(P_{k-1}^k v^{k-1} - P_{k-1}^k \hat{v}^{k-1}) + \tilde{G}_k(\tilde{d}^k - \hat{d}^k) \\ &= \tilde{H}_k(D_k^{k-1} P_{k-1}^k v^{k-1} - D_k^{k-1} P_{k-1}^k \hat{v}^{k-1}) + \tilde{G}_k(\tilde{d}^k - \hat{d}^k) \\ &= \tilde{H}_k(v^{k-1} - \hat{v}^{k-1}) + \tilde{G}_k(\tilde{d}^k - \hat{d}^k). \end{aligned}$$

Now by definitions of α, β, and $\hat{d}^k = \mathrm{tr}(\tilde{d}^k, \epsilon_k)$, it follows that

$$\begin{aligned} \left\| v^k - \hat{v}^k \right\| &\le \left\| \tilde{H}_k(v^{k-1} - \hat{v}^{k-1}) \right\| + \left\| \tilde{G}_k(\tilde{d}^k - \hat{d}^k) \right\| \\ &\le \alpha \left\| v^{k-1} - \hat{v}^{k-1} \right\| + \beta\epsilon_k. \end{aligned}$$

Applying this bound recursively,

$$\left\| v^L - \hat{v}^L \right\| \;\le\; \beta \sum_{k=1}^{L} \alpha^{L-k} \epsilon_k \;=\; \beta\epsilon \frac{1 - (\alpha q)^L}{1 - \alpha q} \;<\; \frac{\beta\epsilon}{1-\alpha q}. \qquad \square$$

COROLLARY 5.2. *Let $\|v\|$ be the scaled ℓ^p norm $J_k^{-1/p} \|v\|_p$. Let $\tilde{h}$ and $\tilde{g}$ be wavelet filters as in section 4.1, and let $\tilde{h}_n^e = \tilde{h}_{2n}$ and $\tilde{h}_n^o = \tilde{h}_{2n+1}$ be the even and odd components of $\tilde{h}$, and similarly $\tilde{g}^e$ and $\tilde{g}^o$ be the even and odd components of $\tilde{g}$.*

Suppose that $\circledast$ is periodic convolution or, for convolution with other boundary handling, suppose that the wavelet filters have the form $h(z) = h_0 + zh^o(z^2)$ and $g(z) = z^{-1}$. Then $\tilde{H}_k v = \tilde{h} \circledast \uparrow v$ and $\tilde{G}_k v = \tilde{g} \circledast \uparrow v$.

(i) *If $\circledast$ is periodic convolution, then Theorem* 5.1 *applies with*

(5.5)
$$\alpha = \left(\frac{\|\tilde{h}^e\|_1^p + \|\tilde{h}^o\|_1^p}{2} \right)^{1/p}, \quad \beta = \left(\frac{\|\tilde{g}^e\|_1^p + \|\tilde{g}^o\|_1^p}{2} \right)^{1/p} \quad \text{if } 1 \le p < \infty,$$
$$\alpha = \|\tilde{h}^e\|_1 \vee \|\tilde{h}^o\|_1, \qquad \beta = \|\tilde{g}^e\|_1 \vee \|\tilde{g}^o\|_1 \qquad \text{if } p = \infty.$$

(ii) *If $\circledast$ is zero-padded convolution and $h(z) = h_0 + zh^o(z^2)$, $g(z) = z^{-1}$, then Theorem* 5.1 *applies with* (5.5).

(iii) *If $\circledast$ is convolution with symmetric or constant boundary extension and $h(z) = h_0 + zh^o(z^2)$, $g(z) = z^{-1}$, then Theorem* 5.1 *applies with* (5.5) *for $p = \infty$.*

Proof. (i) By Young's inequality on the periodic grid,

$$\begin{aligned} J_k^{-1/p} \left\| \tilde{h} \circledast \uparrow v \right\|_p &= J_k^{-1/p} \left[\left\| \tilde{h}^e \circledast v \right\|_p^p + \left\| \tilde{h}^o \circledast v \right\|_p^p \right]^{1/p} \\ &\le J_k^{-1/p} \left[\left(\left\| \tilde{h}^e \right\|_1^p + \left\| \tilde{h}^o \right\|_1^p \right) \|v\|_p^p \right]^{1/p} = \alpha J_{k-1}^{-1/p} \|v\|_p . \end{aligned}$$

(ii) and (iii) Let $v \in V^k$, and let v^{ext} be its extension to the infinite grid, as determined by the boundary-handling method, but with $v_n^{\text{ext}} = 0$ for $|n| > \operatorname{supp} \tilde{h} + \operatorname{supp} v$. Then $(\tilde{h} \circledast \uparrow v)_n = (\tilde{h} * \uparrow \tilde{v})_n$ for $n = 0, \dots J_k - 1$ and $\|v\|_p = \|v^{\text{ext}}\|_p$. By Young's inequality on the infinite grid,

$$\begin{aligned} J_k^{-1/p} \left\| \tilde{h} \circledast \uparrow v \right\|_p &\le J_k^{-1/p} \left\| \tilde{h} * \uparrow v^{\text{ext}} \right\|_p \\ &= J_k^{-1/p} \left[\left\| \tilde{h}^e * v^{\text{ext}} \right\|_p^p + \left\| \tilde{h}^o * v^{\text{ext}} \right\|_p^p \right]^{1/p} \\ &\le J_k^{-1/p} \left[\left(\left\| \tilde{h}^e \right\|_1^p + \left\| \tilde{h}^o \right\|_1^p \right) \left\| v^{\text{ext}} \right\|_p^p \right]^{1/p} = \alpha J_{k-1}^{-1/p} \|v\|_p . \end{aligned}$$

Similarly, β is such that $\left\| \tilde{g} \circledast v \right\| \le \beta \|v\| \le \beta \|v\|_\infty$. ∎

Remark 8. For nonperiodic boundary handling, the requirement $h(z) = h_0 + zh^o(z^2)$ and $g(z) = z^{-1}$ ensures a wavelet transform implementation with a single update lifting step. For wavelets with more than one lifting step, it is generally not true that $\tilde{H}_k v = \tilde{h} \circledast \uparrow v$ and $\tilde{G}_k v = \tilde{g} \circledast \uparrow v$, though these formulas do hold for points sufficient far from the boundaries.

However, presuming these boundary effects are small, the conclusions of Theorem 5.1 with (5.5) hold approximately for any wavelet and boundary handling.

For the point-value, cell-average, and hat-based discretizations, the wavelet filters have the form $h(z) = h_0 + zh^o(z^2)$ and $g(z) = z^{-1}$. For both the cell-average and hat-based discretizations with periodic or zero-padded boundary handling, $\alpha = 2^{1-1/p}$ and $\beta = 1$, and Theorem 5.1 yields

$$J_L^{-1/p} \left\| v^L - \hat{v}^L \right\|_p \le \frac{\epsilon}{1 - 2^{1-1/p} q} = \begin{cases} \dfrac{\epsilon}{1-q} & \text{for } p = 1, \\ \dfrac{\epsilon}{1-\sqrt{2}q} & \text{for } p = 2, \\ \dfrac{\epsilon}{1-2q} & \text{for } p = \infty. \end{cases}$$

For cell-average discretization, this bound agrees with (5.3) for $p = 1$ and is worse for $p = 2, \infty$. For hat-based discretization, it agrees with (5.4) for $p = \infty$ and is better for $p < \infty$.

For point-value discretization, Theorem 5.1 is overly conservative with error bound $\epsilon/(2^{1/p-1} - q)$, which is much worse than (5.2). However, this case is extreme, as all involved filters are one-tap.

6. Example constructions. In this section, two examples of Harten multiresolution schemes are constructed using the approach proposed in the previous sections. The first is a family of spline discretization schemes, where cell-average discretization is order $N = 1$ and hat-based discretization is $N = 2$. The second is a simple example with nonspline decimation filters.

6.1. Spline discretizations. This section develops Harten schemes with spline discretization. Let $h(z)$ be the Nth-order spline decimation filter

$$h(z) = z^{\lfloor N/2 \rfloor} \left(\frac{1 + z^{-1}}{2} \right)^N,$$

and define $D_k^{k-1} v^k = {\downarrow}(h * v^k)$. As in section 4.3, the prediction operator is $P_{k-1}^k v^{k-1} = a * Q_{k-1}^k (b * v^{k-1})$ for any interpolatory operator Q_{k-1}^k, with

$$b(z) = \frac{1}{z^{\lfloor N/2 \rfloor}(1 - z^{-1})^N}, \qquad a(z) = z^{\lfloor N/2 \rfloor}(1 - z^{-1})^N.$$

Choose $\tilde{N}$ such that $M = \frac{1}{2}(N + \tilde{N}) - 1$ is integer, and define $\tilde{h}$, g, and $\tilde{g}$ as in (4.4),

$$\tilde{h}(z) = 2z^{\lceil \tilde{N}/2 \rceil} \left(\frac{1 + z^{-1}}{2} \right)^{\tilde{N}} \sum_{n=0}^{M} \binom{M+n}{n} (-4)^{-n} (z - 2 + z^{-1})^n,$$
$$g(z) = \tfrac{1}{2} z^{-1} \tilde{h}(-z), \qquad \tilde{g}(z) = 2z h(-z).$$

The detail encoder operator is $G_k e^k = {\downarrow}(g * e^k)$, and the decoder is $\tilde{G}_k d^k = \tilde{g} * ({\uparrow} d^k)$. At this point, all of the necessary operators for a discrete implementation of the scheme are established.

Now consider the continuous operators $\mathcal{D}_k$ and $\mathcal{R}_k$. The function $\phi(x)$ satisfying dilation equation (4.11) is the B-spline

$$\phi(x) = \frac{1}{(N-1)!} \sum_{n=0}^{N} \binom{N}{n} (-1)^n \left[(x + \left\lfloor \frac{N}{2} \right\rfloor - n)^+ \right]^{N-1}. \tag{6.1}$$

The B-spline ϕ can be shown to satisfy the dilation equation in the Fourier domain. Let $\tau = 0$ if N is even and $\tau = 1$ if N is odd. Its Fourier transform is $\hat{\phi}(\omega) = \mathrm{e}^{-i\omega\tau/2} (\frac{\sin(\omega/2)}{\omega/2})^N$, so that

$$\begin{aligned}
2 \sum_n h_n \tfrac{1}{2} \hat{\phi}(\omega/2) \mathrm{e}^{-in\omega/2} &= 2 \sum_{n=-\lfloor N/2 \rfloor}^{\lceil N/2 \rceil} 2^{-N} \binom{N}{n + \lfloor \frac{N}{2} \rfloor} \tfrac{1}{2} \mathrm{e}^{-i\omega(\tau+2n)/4} \left(\frac{\sin(\omega/4)}{\omega/4} \right)^N \\
&= \mathrm{e}^{-i\omega(\tau - 2\lfloor N/2 \rfloor)/4} \left(\sum_{n=0}^{N} \binom{N}{n} \mathrm{e}^{-i\omega n/2} \right) \left(\frac{\sin(\omega/4)}{\omega/2} \right)^N \\
&= \mathrm{e}^{-i\omega\tau/2} \left(\frac{\sin(\omega/2)}{\omega/2} \right)^N = \hat{\phi}(\omega).
\end{aligned}$$

As in section 4.4, define the discretization operator as $(\mathcal{D}_k f)_n = (\phi_k * f)(x_n^k)$. The primitive $\mathring{f}^k$ is related to f by $\mathring{f}^k = b_{\delta_k} * \phi_k * f$. In the Fourier domain,

$$\hat{b}_{\delta_k}(\omega)\hat{\phi}_k(\omega) \;=\; \frac{\mathrm{e}^{-i\omega\tau/2^{k+1}}\left(\frac{\sin(\omega/2^{k+1})}{\omega/2^{k+1}}\right)^N}{\mathrm{e}^{i\omega(2\lfloor N/2\rfloor - N)/2^{k+1}}(2i\sin(\omega/2^{k+1}))^N} \;=\; 2^{kN}(i\omega)^{-N}. \tag{6.2}$$

Thus the primitive $\mathring{f}^k$ is related to f by an Nth-order integral with scale factor 2^{kN},

$$\mathring{f}^k(x) = 2^{kN}\int_0^x\int_0^{y_1}\cdots\int_0^{y_{N-1}} f(y_N)\,dy_N\cdots dy_2\,dy_1.$$

Let $\mathring{v}_n^k = \mathring{f}^k(x_n^k)$ be samples of $\mathring{f}^k$. In the Fourier domain, ξ_k is

$$\frac{\hat{a}_{\delta_{k+1}}(\omega)}{\hat{\phi}_{k+1}(\omega)} \;=\; \frac{\mathrm{e}^{i\omega(2\lfloor N/2\rfloor - N)/2^{k+2}}(2i\sin(\omega/2^{k+2}))^N}{\mathrm{e}^{-i\omega\tau/2^{k+2}}\left(\frac{\sin(\omega/2^{k+2})}{\omega/2^{k+2}}\right)^N} \;=\; 2^{-kN}(i\omega)^N. \tag{6.3}$$

Convolution with ξ_k is Nth-order differentiation, with a scale factor 2^{-kN}. Given an interpolatory operator $\mathcal{I}_k$, the reconstruction operator is

$$(\mathcal{R}_k v^k)(x) = \big(\xi_k * \mathcal{I}_k(b * v^k)\big)(x) = 2^{-kN}\frac{d^N}{dx^N}(\mathcal{I}_k\mathring{v}^k)(x).$$

If b is scaled by 2^{kN} and a by 2^{-kN}, then the 2^{kN} scale factor in (6.2) and (6.3) cancels, yielding a primitive independent of k:

$$\mathring{f}(x) = \int_0^x\int_0^{y_1}\cdots\int_0^{y_{N-1}} f(y_N)\,dy_N\cdots dy_2\,dy_1,$$
$$(\mathcal{R}_k v^k)(x) = \frac{d^N}{dx^N}(\mathcal{I}_k\mathring{v}^k)(x), \qquad \mathring{v}_n^k = \mathring{f}(x_n^k).$$

Since the primitive $\mathring{f}$ is related to f by Nth-order integration, predicting a polynomial of degree K requires interpolation, with an order of at least $K+N$.

To control regularity, $\mathcal{I}_k\mathring{v}^{k-1}$ should be at least N times weakly differentiable. An ENO interpolant has a weak first derivative, so $\mathcal{I}_k = \mathcal{I}_k^{\mathrm{ENO}}$ works directly for the point-value $N=0$ and the cell-average $N=1$ cases. In the hat-based case $N=2$, the second derivative of an ENO interpolant contains Dirac measures. Aràndiga, Donat, and Harten [6] control the manifestation of Dirac measures in their hat-based scheme using a careful subcell-resolution scheme.

Another solution is to follow P^{ENO} with a smoothing step (4.10). This modification controls the regularity without losing the prediction's edge-adaptive behavior, as demonstrated in Figure 6.1.

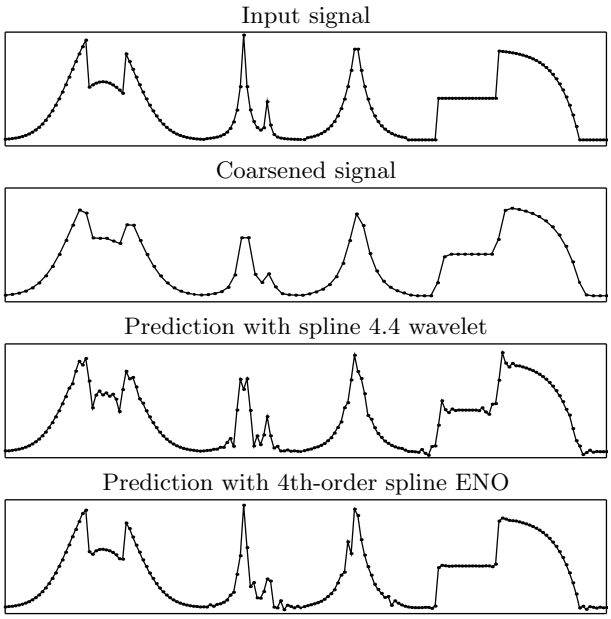

FIG. 6.1. *A piecewise-regular signal is first coarsened with 4th-order spline decimation, and then prediction with the spline 4.4 wavelet and 4th-order spline ENO both attempt to recover the original. ENO interpolation is followed by* (4.10) *to control regularity.*

The hierarchical stencil selection method (described in section 3.1) has the problem that it may select singularity-crossing stencils for discontinuities in $\mathring{f}''$ and higher derivatives [5]. Since a jump becomes a discontinuity in $\mathring{f}^{(N)}$, jump discontinuity in f is not correctly handled for $N \geq 2$. Nonhierarchical selection does not have this problem, so it is the better method for $N \geq 2$.

6.2. A nonspline scheme. Harten's multiresolution framework generalizes wavelets, including those with nonspline lowpass filters. This section constructs a simple Harten multiresolution scheme based on piecewise polyharmonic (PPH) interpolation and the Cohen–Daubechies–Feauveau 9/7 (CDF 9/7) wavelet.

Define the linear/cubic PPH interpolatory operator

$$(P^{\mathrm{PPH}} v)_{2n+1} = \frac{v_{n+1} + v_n}{2} - \frac{1}{4} \frac{(\Delta^2 v_{n+1} \Delta^2 v_n)^+}{\Delta^2 v_{n+1} + \Delta^2 v_n},$$

where $\Delta^2 v_n = v_{n+1} - 2v_n + v_{n-1}$. Amat et al. [3, 4] considered it as the prediction operator in point-value discretization schemes and have shown its nice properties and potential in nonlinear approximation.

Let H, G, $\tilde{H}$, and $\tilde{G}$ be the decomposition and reconstruction operators for the CDF 9/7 wavelet, and let $D_k^{k-1} = H$ be the decimation operator. As in (4.8), a consistent prediction based on P^{PPH} is

$$P_{k-1}^k v^{k-1} = \tilde{H} v^{k-1} + \tilde{G} G P^{\mathrm{PPH}} v^{k-1}. \tag{6.4}$$

The CDF 9/7 PPH scheme is applied to nonlinear approximation in Figure 6.2. An image is sparsely decomposed with 3% nonzero coefficients using the modified encoding algorithm (section 5) and then reconstructed. The same is done with the

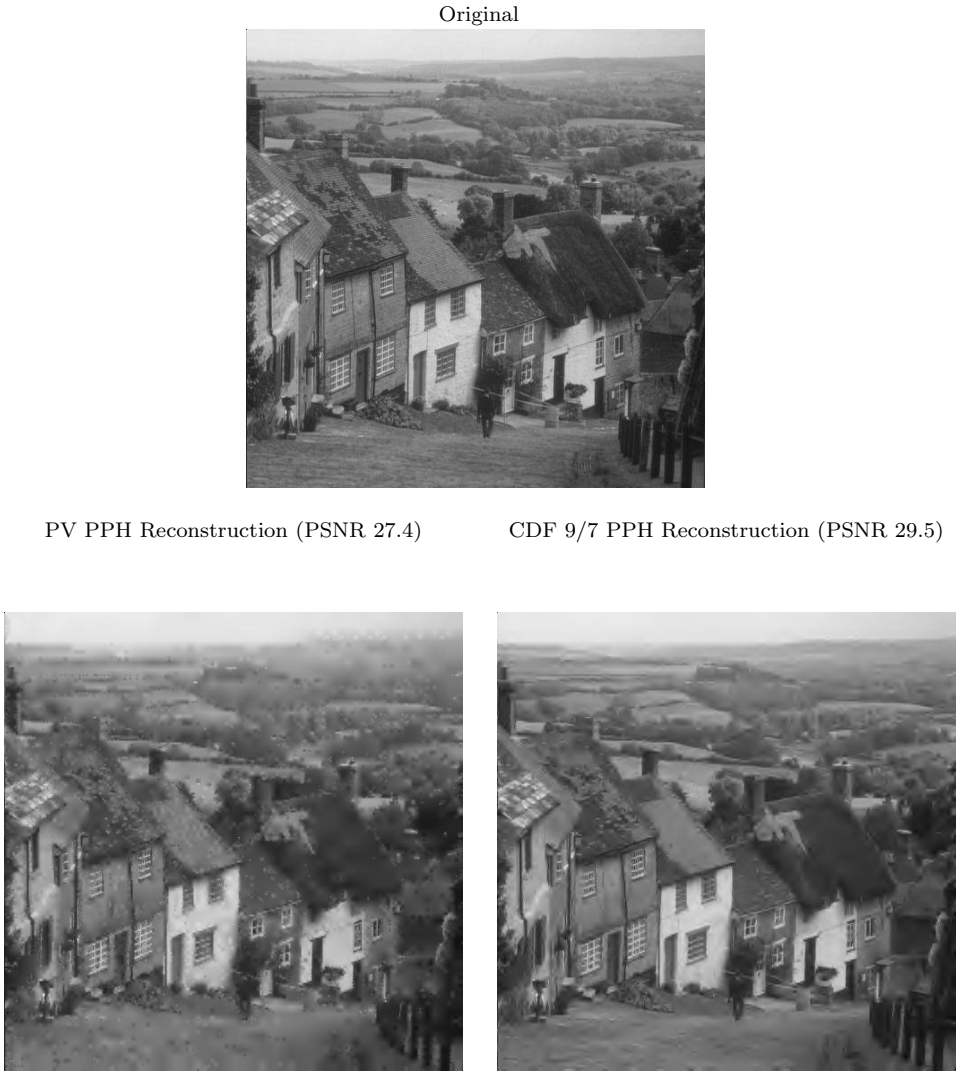

FIG. 6.2. *A nonlinear approximation of Goldhill using* 3% *nonzero coefficients. Left: Reconstruction using point-value discretization and PPH interpolation. Right: Reconstruction using CDF* 9/7 *wavelet discretization and* (6.4).

PPH scheme based on point-value discretization (PV PPH). Reconstruction quality is measured in terms of peak signal-to-noise (PSNR). Since the CDF 9/7 PPH scheme applies a smoothing filter before decimating, it can suppress aliasing artifacts and handle texture better.

7. Conclusion. This paper develops a new approach to the construction of Harten multiresolution schemes, where the decimation operator is based on an arbitrary FIR decimation filter h.

- It is possible to design all of the operators (D_k^{k-1}, P_{k-1}^k, G_k, $\tilde{G}_k$) necessary for implementing a nonredundant decomposition from h without ever defining $\mathcal{D}_k$ or $\mathcal{R}_k$ (section 4.3, section 4.1).

- $\mathcal{D}_k$ and $\mathcal{R}_k$ can be constructed (section 4.4) such that they are consistent with the decimation and prediction operators defined in section 4.3.
- The construction of $\mathcal{R}_k$ "via primitive function" [6, 14], and the notion of primitive generalizes to discretizations with any h (section 4.4).
- Schemes under this construction may be applied to nonlinear approximation using the error-control strategy developed in section 5.
- As a special case, the construction yields a family of Harten schemes with spline discretizations (section 6.1), where the point-value, cell-average, and hat-based discretizations are the first three members.
- It is also possible to construct Harten schemes with nonspline discretizations, as demonstrated by the example in section 6.2.

The presented construction expands the choice of discretization to any discretization with an FIR decimation filter. New Harten multiresolution schemes are possible using smoother and nonspline decimation filters.

Acknowledgments. We are grateful to the reviewers for their comments which helped improve the paper. We also thank Dr. James Curry and Dr. Anne Dougherty, who provided advice and guidance that focused the direction and ensured the quality of this work.

REFERENCES

[1] R. Abgrall and T. Sonar, *On the use of Mühlbach expansions in the recovery step of ENO methods*, Numer. Math., 76 (1997), pp. 1–25.
[2] S. Amat, F. Aràndiga, A. Cohen, R. Donat, G. Garcia, and M. Von Oehsen, *Data compression with ENO schemes: A case study*, Appl. Comput. Harmon. Anal., 11 (2002), pp. 273–288.
[3] S. Amat, R. Donat, J. Liandrat, and J.C. Trillo, *A fully adaptive PPH multi-resolution scheme for image processing*, Math. Comput. Modelling, 46 (2007), pp. 2–11.
[4] S. Amat, R. Donat, J. Liandrat, and J.C. Trillo, *Analysis of a new nonlinear subdivision scheme*, Applications in image processing, Found. Comp. Math., 6 (2006), pp. 193–225.
[5] F. Aràndiga and R. Donat, *Nonlinear multiscale decompositions: The approach of A. Harten*, Numer. Algorithms, 23 (2000), pp. 175–216.
[6] F. Aràndiga, R. Donat, and A. Harten, *Multiresolution based on weighted averages of the hat function* II: *Nonlinear reconstruction techniques*, SIAM J. Sci. Comput., 20 (1998), pp. 1053–1093.
[7] T. Cecil, J. Qian, and S. Osher, *Numerical methods for high dimensional Hamilton-Jacobi equations using radial basis functions*, J. Comput. Phys., 2003.
[8] R. Claypoole, G. Davis, W. Sweldens, and R. Baraniuk, *Nonlinear wavelet transforms for image coding*, in Proceedings of the 31st IEEE Asilomar Conference, Pacific Grove, CA, 1997.
[9] A. Cohen and B. Mateï, *Compact representation of images by edge adapted multiscale transforms*, in Proceedings of the International Conference on Image Processing, Thessaloniki, Greece, IEEE, 2001.
[10] A. Cohen, N. Dyn, and B. Mateï, *Quasilinear subdivision schemes with applications to ENO interpolation*, Appl. Comput. Harmon. Anal., 15 (2003), pp. 89–116.
[11] S. Godavarthy, *Generating spline wavelets*, in Proceedings in the 36th ACM Southeast Regional Conference, Marietta, GA, 1998, pp. 8–14.
[12] A. Harten, B. Engquist, S. Osher, and S. Chakravarthy, *Uniformly high order accurate essentially non-oscillatory schemes* III, J. Comput. Phys., 71 (1987), pp. 231–303.
[13] A. Harten, *Discrete multiresolution analysis and generalized wavelets*, J. Appl. Numer. Math., 12 (1993), pp. 152–192.
[14] A. Harten, *Multiresolution representation of data*: *A general framework*, SIAM J. Numer. Anal., 33 (1996), pp. 1205–1256.
[15] H. Heijmans and J. Goutsias, *Nonlinear multiresolution signal decomposition schemes–Part* II: *Morphological wavelets*, IEEE Trans. Image Process., 9 (2000), pp. 1897–1913.

[16] A. Iske and T. Sonar, *On the structure of function spaces in optimal recovery of point functionals for ENO-schemes by radial basis functions*, Numer. Math., 74 (1996), pp. 177–201.
[17] S. Mallat, *A Wavelet Tour of Signal Processing*, Academic Press, New York, 1998.
[18] T. Sonar, *On families of pointwise optimal finite volume ENO approximations*, SIAM J. Numer. Anal., 35 (1998), pp. 2350–2369.
[19] W. Sweldens, *The lifting scheme: A construction of second generation wavelets*, SIAM J. Math. Anal., 29 (1998), pp. 511–546.